Interplay of Electronic and Spin Degrees in Ferromagnetic $SrRuO_3$: Anomalous Softening of the Magnon Gap and Stiffness

K. Jenni,[1] S. Kunkemöller,[1] D. Brüning,[1] T. Lorenz,[1] Y. Sidis,[2] A. Schneidewind,[3] A. A. Nugroho,[4] A. Rosch,[5] D. I. Khomskii,[1] and M. Braden[1,*]

[1]*II. Physikalisches Institut, Universität zu Köln, Zülpicher Str. 77, D-50937 Köln, Germany*
[2]*Laboratoire Léon Brillouin, C.E.A./C.N.R.S., F-91191 Gif-sur-Yvette CEDEX, France*
[3]*Jülich Centre for Neutron Science (JCNS) at Heinz Maier-Leibnitz Zentrum (MLZ), Forschungszentrum Jülich GmbH, Lichtenbergstraße 1, 85748 Garching, Germany*
[4]*Faculty of Mathematics and Natural Science, Institut Teknologi Bandung, Jalan Ganesha 10, 40132 Bandung, Indonesia*
[5]*Institut für Theoretische Physik, Universität zu Köln, Zülpicher Str. 77a, D-50937 Köln, Germany*

(Received 11 February 2019; published 3 July 2019)

The magnon dispersion of ferromagnetic $SrRuO_3$ was studied by inelastic neutron scattering experiments on single crystals as a function of temperature. Even at low temperature the magnon modes exhibit substantial broadening pointing to strong interaction with charge carriers. We find an anomalous temperature dependence of both the magnon gap and the magnon stiffness, which soften upon cooling in the ferromagnetic phase. Both effects trace the temperature dependence of the anomalous Hall effect and can be attributed to the impact of Weyl points, which results in the same relative renormalization in the spin stiffness and magnon gap.

DOI: 10.1103/PhysRevLett.123.017202

Strong spin-orbit coupling (SOC) causes intertwining of charge and spin degrees of freedom, which may result in various fascinating phenomena such as Weyl semimetals [1–3], multiferroics [4], or spin liquids with exotic excitations [5,6]. For a ferromagnetic metal the combination of magnetic exchange with strong SOC splits the bands and causes the emergence of Weyl points. These Weyl points possess strong impact not only on the charge transport [7] but also on the magnetic properties. The anomalous Hall effect can capture the impact of the Weyl points on the charge dynamics. As we will show below, the same physics influences also directly the magnon dispersion: the magnon anisotropy gap [8] and stiffness.

$SrRuO_3$ [9–11] with the $4d$ ion Ru^{4+} is a prime candidate to observe the impact of strong SOC in a ferromagnetic metal. It crystallizes in the cubic perovskite structure but undergoes two structural phase transitions at 975 and 800 K into an orthorhombic phase (space group *Pnma*) associated with rotations of the RuO_6 octahedra [9,12,13]. The ferromagnetic transition occurs at 165 K in our single crystals and at low temperature a magnetization of $\sim 1.6\mu_B$ is observed at 6 T [14]. The electric resistivity is linear at moderate temperatures and breaks the Ioffe-Regel limit, but it drops in the ferromagnetic phase with a clear kink at the ferromagnetic T_c [15,16] attaining very low residual resistivity values of only 3 $\mu\Omega$ cm in high-quality single crystals [14,17]. This coupling of ferromagnetic excitations and charge transport inspired the proposal of spin-triplet pairing in the superconducting sister compound Sr_2RuO_4 [18], in which quasiferromagnetic excitations could only recently be observed in neutron experiments [19]. The anomalous Hall effect in $SrRuO_3$ shows a peculiar temperature dependence undergoing a sign change [7,8,11,20–22]. Fang *et al.* [7] proposed that the anomalous Hall effect in $SrRuO_3$ arises from the impact of magnetic monopoles in momentum space associated with Weyl points. The magnetic exchange splitting combined with the impact of SOC causes Weyl points in the band structure [7,8], which DFT calculations predict to occur near the Fermi level [23].

More recently Itoh *et al.* argued that the Weyl points not only induce the peculiar temperature dependence of the anomalous Hall effect but also affect the spin dynamics. At each Weyl point, index i, two bands cross and the single-particle current $j_n^{W,i} = e\sum_m v_{nm}^i \boldsymbol{\sigma}^m$ and magnetization $m_n^{W,i} = \sum_m g_{nm}^i \mu_B (\hbar\boldsymbol{\sigma}^m/2)$ are proportional to each other [1]

$$\boldsymbol{m}^{W,i} = \frac{\hbar\mu_B}{2e}\boldsymbol{g}^i(\boldsymbol{v}^i)^{-1}\boldsymbol{j}^{W,i}, \tag{1}$$

where $\boldsymbol{g}^i$ is the g tensor, $n, m = x, y, z$, $\boldsymbol{v}^i$ the tensor of Fermi velocities characterizing the Weyl point i, and $\boldsymbol{\sigma}^m$ are the Pauli matrices encoding the two crossing bands. The intimate relation of current, magnetization, and Berry phases will be tested by our Letter.

Inelastic neutron scattering (INS) experiments in Ref. [8] indeed find a temperature dependence of the magnon gap resembling that of the anomalous Hall effect while the magnon stiffness was claimed to exhibit a normal temperature dependence, i.e., a hardening upon cooling. However,

these measurements were performed with powder samples that do not give direct access to the parameters of the magnon dispersion. Here we report on INS, magnetization, and the anomalous Hall effect measurements on single-crystalline $SrRuO_3$. We confirm a close similarity between the temperature dependencies of the magnon gap and the anomalous Hall conductivity, but the magnon gap differs from the powder experiment by almost a factor of 2. Furthermore, the magnon stiffness also softens upon cooling in the ferromagnetic phase in contrast to the powder INS study. We argue that this unusual temperature dependence originates from the coupling of current and magnetization thus confirming the impact of the anomalous Hall effect on magnetization dynamics.

Large single crystals of $SrRuO_3$ were grown by the floating-zone technique and characterized by resistivity and magnetization measurements [14]. For the INS experiments six crystals with a total mass of ~6 g were coaligned in the [100]/[011] scattering plane in respect to the pseudocubic lattice with $a_c \sim 3.92$ Å. INS experiments were performed on cold triple-axis spectrometers (TAS) 4F at the Laboratoire Léon Brillouin and PANDA at the Meier-Leibnitz Zentrum, and on the thermal TAS 2T at the Laboratoire Léon Brillouin. The anomalous Hall effect was measured on a rectangular sample with edge lengths of $2.2 \times 1.64 \times 0.193$ mm^3 along the cubic directions $[1\bar{1}0]$, [001], and [110], respectively. We applied the electrical current I_x (typically 5 mA) along $[1\bar{1}0]$ (orthorhombic a), the external magnetic field along [110] (the easy axis, orthorhombic c, up to ±7 T) and measured the longitudinal ($U_x||I_x$) and the transverse voltage $U_y||[001]$ (orthorhombic b). Using a SQUID magnetometer, we also measured the magnetization M of this sample for the same field direction in order to precisely determine the normal and anomalous Hall effects. Further experimental details are given in the Supplemental Material [24].

Figure 1 shows the INS data obtained by constant energy scans across the magnon dispersion on cold and thermal TAS. The peaks arising from the magnon on both sides of the (100) Bragg points are clearly visible and allow for a reliable determination of the dispersion. In order to quantitatively analyze these data we calculate the folding of the magnon dispersion with the resolution of the cold and thermal TAS using the ResLib program package [25]. The lines superposed to the constant energy scans refer to this folding procedure with only a few global fit parameters. For small momenta, the magnon dispersion can approximately be described by $E_0(\boldsymbol{q}) \approx \Delta + D\boldsymbol{q}^2$, with the anisotropy gap Δ and the magnon stiffness D. Magnetic anisotropy is sizable in $SrRuO_3$ as it can be inferred from the macroscopic magnetic anisotropy [14,26,27] and the shape memory effect [17] and from an optical study [28]. The small orthorhombic distortion of $SrRuO_3$ induces a tiny anisotropy in D, see below. Note, that throughout the Letter we use reduced reciprocal lattice units with respect to the

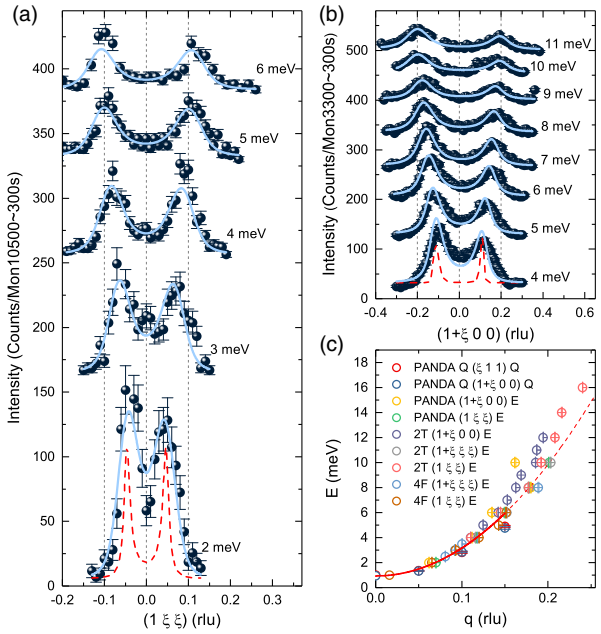

FIG. 1. (a) and (b) Constant energy scans across the magnon dispersion in $SrRuO_3$ at various energies obtained at $T = 10$ K on the cold TAS 4F and on the thermal TAS 2T, respectively. Lines represent the folding of the modeled magnon dispersion including a broadening term with the resolution function of the spectrometer; data are vertically offset for clarity. Dashed lines illustrate the experimental resolution that would describe the data in the absence of any magnon broadening. (c) Combined magnon dispersion traced against the length of the magnon propagation vector $|\vec{q}|$ in relative lattice units. The line reproduces the quadratic low-q behavior defining the magnon stiffness.

pseudocubic cell, $2\pi/a_c$, but the stiffness is typically given in units of meV Å^2. In order to describe the measured scan profiles we need to assume a width of the magnon modes that amounts to 40% of their energy. Part of this broadening can stem from the twinning of the crystals superposing different direction of the orthorhombic lattice, but due to the small orthorhombic distortion this broadening should be of the order of a few percent only. Magnons in $SrRuO_3$ thus exhibit strong scattering most likely due to the coupling to electrons, see also the kink in resistivity at T_c [15,16], and due to the presence of sizable SOC. The dispersion, which for small $|\boldsymbol{q}|$ values is quadratic, is presented in Fig. 1(c). A consistent description of the data at low temperatures is obtained yielding $D = 87(2)$ meV Å^2 and $\Delta = 0.94(3)$ meV and an energy width of $0.4E_0(q)$. Note that the gap Δ is almost a factor of 2 smaller than the result obtained from the powder experiment, and also the stiffness D considerably differs [8].

With the better resolution of the cold TAS 4F we scanned across the magnon gap at the zone center; see Fig. 2. Again the gap can be directly read from the raw data in contrast to the previous powder INS experiment [8]. Our single-crystal INS result further agrees with the optical study [28] and

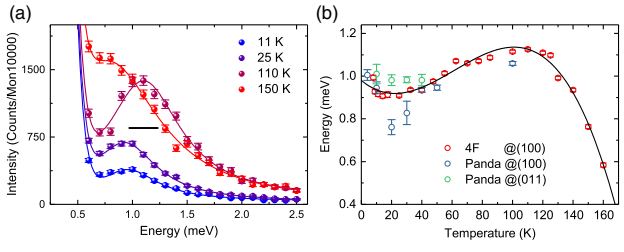

FIG. 2. (a) Energy scans at the magnetic (and nuclear) Brillouin zone center (100) across the magnon gap arising from anisotropy. The data are taken at the cold TAS 4F with final neutron energy of 4.98 meV. The resolution (full width at half maximum) is indicated by the horizontal bar. (b) The resulting gap values as a function of temperature. Data taken on the cold TAS PANDA taken on an untwinned crystal are included; the line is a guide to the eye.

with the extrapolation of the anisotropic magnetization [17]. The easy axis of $SrRuO_3$ is found along the orthorhombic c direction in *Pnma* notation [17] and therefore two anisotropy gaps can be expected for the orthorhombic system, i.e., for rotating the magnetic moments towards the a and b directions. Our data indicate little splitting for the two gaps that were examined with an untwinned smaller crystal on PANDA. This crystal was first mechanically detwinned [14] and then mounted with its cubic $[01\bar{1}]$ direction parallel to a magnetic field in a vertical field cryostat. After applying a magnetic field of 3 T a fully monodomain crystal was obtained [17] with the orthorhombic c axis, the magnetic easy axis, parallel to cubic $[01\bar{1}]$, and thus $a\|[011]$ and $b\|[100]$. The gaps measured at the scattering vectors $\mathbf{Q} = (100)$ and (011) correspond thus to the rotation of the moments towards a and b, respectively. In agreement with the macroscopic analysis in Ref. [17] the a direction is only slightly softer than b. The anomalies of the gap temperature dependence are qualitatively confirmed by these monodomain measurements, but the temperature dependence of the averaged gap profits from higher statistics. From the constant $\mathbf{Q}$ scans at the zone center we deduce the temperature dependence of the anisotropy gap by fitting a Gaussian peak; see Fig. 2(b). In only qualitative agreement with the powder INS [8] there is a rather anomalous softening and rehardening of the gap upon cooling deep in the ferromagnetic phase, while the closing of the gap upon heating above the Curie temperature corresponds to the expected behavior.

Figure 3 summarizes the temperature dependence of the magnon stiffness. We recorded constant energy scans at 8 meV between 13 and 280 K that were analyzed by fitting the D value through the folding of the resolution with the dispersion. The characteristic two peak structure remains visible even well above the Curie temperature, which underlines the persistence of ferromagnetic correlations. This scattering agrees with the expectation for a nearly ferromagnetic metal, which still exhibits a paramagnon

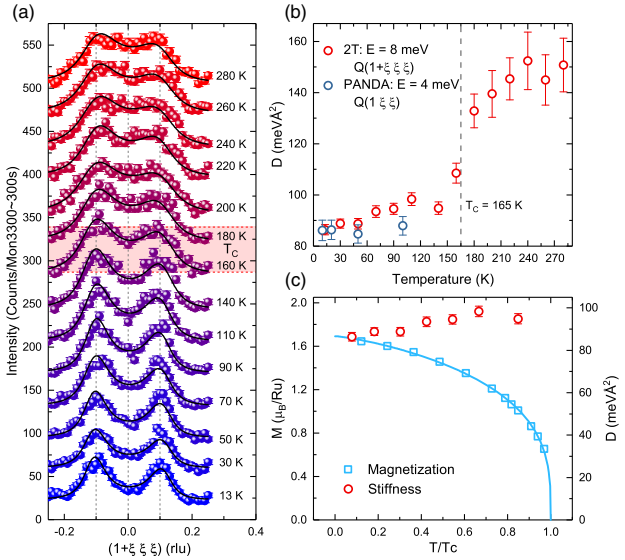

FIG. 3. (a) Constant energy scans across the magnon dispersion in $SrRuO_3$ at 8 meV obtained at the thermal TAS 2T. Lines represent the folding of the magnon dispersion including a broadening term with the resolution function of the spectrometer. (b) Temperature dependence of the magnon stiffness obtained from the data in (a) and from additional measurements on the cold TAS PANDA. Above the ferromagnetic transition D just describes the position of the paramagnon scattering, see text. (c) Comparison of the temperature dependencies of the magnetization and that of the magnon stiffness.

signal very similar to that of the ferromagnetic material with broad magnons [29]. The fitted $\vec{q}$ positions can be directly transformed into temperature-dependent stiffness constants, D, by taking the temperature dependent anisotropy gaps into account, Fig. 3(b). The magnon stiffness clearly softens upon cooling well below the Curie temperature, while the magnetization increases. In Fig. 3(c) we compare the stiffness to the spontaneous magnetization, because in a usual system one expects the two quantities to scale. In contrast, in $SrRuO_3$ the stiffness softens upon cooling well below T_c. Scaling the magnetization M_s and D by the low-temperature values, one recognizes that at 0.8 times T_c the stiffness is almost twice as large as what follows from $D \propto m$. In contrast, the powder INS experiment [8] just reported such a scaling relation for the magnon stiffness [30].

The dynamics of small-amplitude, long-wavelength oscillations of the magnetization in a ferromagnet polarized in the z direction can be described by the action [8]

$$S \approx \frac{1}{2}\int d^3\boldsymbol{r}dt\alpha(T)\left(\frac{dm_x}{dt}m_y - \frac{dm_y}{dt}m_x\right) - \kappa(T)(m_x^2 + m_y^2) - A(T)((\boldsymbol{\nabla}m_x)^2 + (\boldsymbol{\nabla}m_y)^2) + \cdots \tag{2}$$

up to higher order corrections and damping terms. From the corresponding Euler-Lagrange equations one obtains

$$\Delta = \frac{\kappa(T)}{\alpha(T)}, \qquad D = \frac{A(T)}{\alpha(T)}. \tag{3}$$

In the absence of spin-orbit coupling α is exactly given by $\alpha_0 = \{1/[2m(T)\mu_B]\}$, where $m(T)$ is the magnetization density. Taking SOC and the Weyl points into account $\alpha(T)$ is determined not only by $m(T)$ but also by the anomalous Hall effect [8,24]

$$\alpha(T) \approx \frac{1}{g\mu_B m(T)} + c(T)\sigma^a_{xy}(T). \tag{4}$$

This equation arises because the time-dependent magnetization induces currents close to the Weyl points; see Eq. (1) and Ref. [24]. Because of the Berry curvature of the Bloch bands, both a transverse current and a transverse magnetization are generated, modifying $\alpha(T)$.

Neglecting the T dependence of $\kappa(T)$, $c(T)$, and $A(T)$, we obtain from Eqs. (3) and (4) for the spin gap Δ [8] and the stiffness D the same temperature dependence parametrized by

$$\Delta(T) \approx \frac{a_\Delta m(T)/m_0}{1 + b(m(T)/m_0)(\sigma_{xy}(T)/\sigma_0)},$$
$$D(T) \approx \frac{a_D m(T)/m_0}{1 + b(m(T)/m_0)(\sigma_{xy}(T)/\sigma_0)}, \tag{5}$$

where $m_0 = m(T = 0)$ and $\sigma_0 = (e^2/2\pi\hbar a_c)$.

In order to verify the scaling between the anomalous Hall effect and the two characteristic parameters of the magnon dispersion in $SrRuO_3$ we also measured the magnetization and anomalous Hall effect on a single crystal. The magnetization obtained by extrapolating field-dependent magnetization curves to $H = 0$ T is shown in Fig. 3(c) and can be described by a stretched power law $m(T) = m_0[1 - (T/T_c)^a]\beta$ with the parameters $m_0 = 1.69\mu_B$, $a = 1.27$, and $\beta = 0.304$. The field-dependent magnetization was inserted in the analysis of the anomalous Hall effect measurement performed on the same sample. The comparison of our and previous Hall conductivity results is shown in Figs. 4(a) and 4(b). Because of the larger thickness of the single-crystalline sample the Hall voltage is smaller, but it offers the advantage of more precise magnetization data. Our single-crystal data of the Hall conductivity σ_{xy} agree with previous single-crystal data but only qualitatively with powder and thin film data [8,31]. There is a sign change in σ_{xy} slightly below the ferromagnetic transition. Differences may stem from the twinning and different orientations of the distorted orthorhombic lattices in the powder and thin-film experiments and from differences in sample quality. The temperature dependence of the anomalous Hall effect was fitted by a polynomial and then inserted in Eq. (5) to describe the anomalous softening of the magnon gap in the ferromagnetic phase; see Fig. 4(b). This analysis well reproduces the main

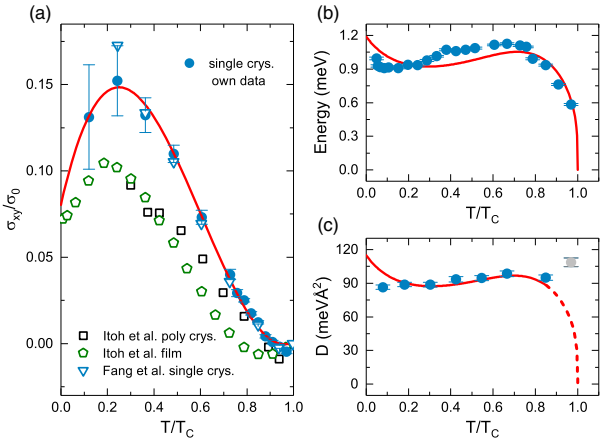

FIG. 4. Comparison of the anomalous Hall effect with the magnon gap and stiffness. (a) Temperature dependence of the anomalous Hall effect normalized to σ_0 measured on single crystals and analyzed with the magnetization curves obtained on the same samples [31]. (b) Temperature dependence of the magnon gap (circles) compared to that of the anomalous Hall effect described by the relation (5). (c) Temperature dependence of the magnon stiffness analyzed in comparison to the anomalous Hall effect, relation (5).

feature with $a_\Delta = 1.66$ meV and $b = 4.98$. The same temperature dependence of the anomalous Hall effect was used to describe the softening of the stiffness compared to a normal behavior proportional to the magnetization, $a_D = 160.90$ meV Å^2. Again good agreement is obtained, see Fig. 4(c). Taking into account that Eq. (5) completely neglects corrections arising, e.g., from the T and magnetization dependence of $K(T)$, $A(T)$, $c(T)$ and from the broadening of the spin waves, the semiquantitative agreement is satisfactory. The temperature dependencies of these entities should be below 10%, while the entire renormalization amounts to about 50%. We emphasize, that the identical correction, i.e., the same b value, describes the deviation of both the gap and the stiffness from being proportional to the magnetization. This clearly supports a common origin of the unusual softening of spin gap and spin stiffness towards lower temperatures, explained by the coupling of magnetization and current and by the T dependence of the anomalous Hall effect.

At the phase transition, where $m(T)$ vanishes, Eq. (5) predicts that $D(T)$ vanishes also. However, in this temperature regime the broad spin waves smoothly transform into paramagnon scattering [29] with a very similar shape and thus a drop of $D(T)$ cannot be extracted from the measured neutron scattering data.

In conclusion, we have studied the magnetization, anomalous Hall effect, and magnon dispersion in $SrRuO_3$ using high-quality single crystals. The magnon modes exhibit sizable broadening, revealing strong scattering by most likely charge carriers. The magnon gap and the magnon stiffness do not follow the temperature dependence

of the spontaneous magnetization. Both quantities soften upon cooling over a large temperature range in the ferromagnetic phase and at least the magnon gap passes through a minimum. These findings can be well explained by the effect of Weyl points situated close to the Fermi level. Such Weyl points possess a well-established impact on the anomalous Hall effect and cause an additional term in the magnetic Hamiltonian. The latter leads to a reduction of both the magnon gap and the stiffness, which scales with the anomalous Hall effect. Our data agree with this scaling between the anomalous Hall effect and the magnon dispersion.

We thank I. Lindfors-Vrejoiu for discussions. This work was funded by the Deutsche Forschungsgemeinschaft (DFG, German Research Foundation)—Project No. 277146847—CRC 1238, projects A02, B01, B04, C02, and C04.

*braden@ph2.uni-koeln.de

[1] A. A. Burkov and L. Balents, Phys. Rev. Lett. **107**, 127205 (2011).
[2] X. Wan, A. M. Turner, A. Vishwanath, and S. Y. Savrasov, Phys. Rev. B **83**, 205101 (2011).
[3] S. Murakami, New J. Phys. **9**, 356 (2007).
[4] D. Khomskii, Physics **2**, 20 (2009).
[5] A. Kitaev, Ann. Phys. (Amsterdam) **321**, 2 (2006).
[6] J. c. v. Chaloupka, G. Jackeli, and G. Khaliullin, Phys. Rev. Lett. **105**, 027204 (2010).
[7] Z. Fang, N. Nagaosa, K. S. Takahashi, A. Asamitsu, R. Mathieu, T. Ogasawara, H. Yamada, M. Kawasaki, Y. Tokura, and K. Terakura, Science **302**, 92 (2003).
[8] S. Itoh, Y. Endoh, T. Yokoo, S. Ibuka, J.-G. Park, Y. Kaneko, K. S. Takahashi, Y. Tokura, and N. Nagaosa, Nat. Commun. **7**, 11788 (2016).
[9] J. J. Randall and R. Ward, J. Am. Chem. Soc. **81**, 2629 (1959).
[10] A. Callaghan, C. W. Moeller, and R. Ward, Inorg. Chem. **5**, 1572 (1966).
[11] G. Koster, L. Klein, W. Siemons, G. Rijnders, J. S. Dodge, C.-B. Eom, D. H. A. Blank, and M. R. Beasley, Rev. Mod. Phys. **84**, 253 (2012).
[12] C. W. Jones, P. D. Battle, P. Lightfoot, and W. T. A. Harrison, Acta Crystallogr. Sect. C **45**, 365 (1989).
[13] B. Chakoumakos, S. Nagler, S. Misture, and H. Christen, Physica (Amsterdam) **241–243B**, 358 (1997).
[14] S. Kunkemöller, F. Sauer, A. A. Nugroho, and M. Braden, Cryst. Res. Technol. **51**, 299 (2016).
[15] P. B. Allen, H. Berger, O. Chauvet, L. Forro, T. Jarlborg, A. Junod, B. Revaz, and G. Santi, Phys. Rev. B **53**, 4393 (1996).
[16] L. Klein, J. S. Dodge, C. H. Ahn, G. J. Snyder, T. H. Geballe, M. R. Beasley, and A. Kapitulnik, Phys. Rev. Lett. **77**, 2774 (1996).
[17] S. Kunkemöller, D. Brüning, A. Stunault, A. A. Nugroho, T. Lorenz, and M. Braden, Phys. Rev. B **96**, 220406(R) (2017).
[18] T. M. Rice and M. Sigrist, J. Phys. Condens. Matter **7**, L643 (1995).
[19] P. Steffens, Y. Sidis, J. Kulda, Z. Q. Mao, Y. Maeno, I. I. Mazin, and M. Braden, Phys. Rev. Lett. **122**, 047004 (2019).
[20] M. Izumi, K. Nakazawa, Y. Bando, Y. Yoneda, and H. Terauchi, J. Phys. Soc. Jpn. **66**, 3893 (1997).
[21] Y. Kats, I. Genish, L. Klein, J. W. Reiner, and M. R. Beasley, Phys. Rev. B **70**, 180407(R) (2004).
[22] N. Haham, Y. Shperber, M. Schultz, N. Naftalis, E. Shimshoni, J. W. Reiner, and L. Klein, Phys. Rev. B **84**, 174439 (2011).
[23] Y. Chen, D. L. Bergman, and A. A. Burkov, Phys. Rev. B **88**, 125110 (2013).
[24] See Supplemental Material at http://link.aps.org/supplemental/10.1103/PhysRevLett.123.017202 for additional information about experimental details and about the calculation.
[25] Reslib-manual, Reslib, http://www.neutron.ethz.ch/research/resources/reslib.html, Neutron Scattering Sciences Division, Oak Ridge National Laboratory, Oak Ridge, 2007.
[26] A. Kanbayasi, J. Phys. Soc. Jpn. **41**, 1876 (1976).
[27] G. Cao, S. McCall, M. Shepard, J. E. Crow, and R. P. Guertin, Phys. Rev. B **56**, R2916 (1997).
[28] M. C. Langner, C. L. S. Kantner, Y. H. Chu, L. M. Martin, P. Yu, J. Seidel, R. Ramesh, and J. Orenstein, Phys. Rev. Lett. **102**, 177601 (2009).
[29] T. Moriya, *Spin Fluctuations in Itinerant Electron Magnetism* (Springer-Verlag, Berlin Heidelberg, 1985).
[30] The discrepancies between our and the previous powder INS results seem to arise from a bad definition of the magnon signal in the powder experiment, where it remains hidden in the elastic line.
[31] Note that there is an inconsistency in the sign of the AHE data published on $SrRuO_3$. In the low-temperature range the AHE is parallel to the normal Hall effect, which corresponds to electron charge carriers, and therefore $\sigma_{xy} \approx -(\rho_{xy}/\rho_{xx}^2)$ is positive in our notation.